Available online at www.sciencedirect.com
SCIENCE DIRECT®
Journal of Applied Geophysics 54 (2003) 203–218
JOURNAL OF APPLIED GEOPHYSICS
www.elsevier.com/locate/jappgeo

Elastic properties of saturated porous rocks with aligned fractures

Boris Gurevich*

Department of Exploration Geophysics, Curtin University of Technology, GPO Box U1987, Perth WA 6845, Australia

Received 5 July 2002; received in revised form 5 November 2002; accepted 6 November 2002

Abstract

Elastic properties of fluid saturated porous media with aligned fractures can be studied using the model of fractures as linear-slip interfaces in an isotropic porous background. Such a medium represents a particular case of a transversely isotropic (TI) porous medium, and as such can be analyzed with equations of anisotropic poroelasticity. This analysis allows the derivation of explicit analytical expressions for the low-frequency elastic constants and anisotropy parameters of the fractured porous medium saturated with a given fluid. The five elastic constants of the resultant TI medium are derived as a function of the properties of the dry (isotropic) background porous matrix, fracture properties (normal and shear excess compliances), and fluid bulk modulus. For the particular case of penny-shaped cracks, the expression for anisotropy parameter ϵ has the form similar to that of Thomsen [Geophys. Prospect. 43 (1995) 805]. However, contrary to the existing view, the compliance matrix of a fluid-saturated porous-fractured medium is not equivalent to the compliance matrix of any equivalent solid medium with a single set of parallel fractures. This unexpected result is caused by the wave-induced flow of fluids between pores and fractures.
© 2003 Elsevier B.V. All rights reserved.

Keywords: Fractures; Anisotropy; Poroelasticity

1. Introduction

Naturally fractured reservoirs have attracted increasing interest in exploration and production geophysics in recent years. In many instances, natural fractures control the permeability of the reservoir, and hence the ability to find and characterize naturally fractured areas of the reservoir represents a major challenge for seismic investigations.

One of the main issues in the characterization of any reservoir is the ability to predict the effect of fluid properties on seismic characteristics. For isotropic porous reservoirs, this effect is expressed through Gassmann's equations, which provide explicit analytical expressions for the elastic moduli of a fluid-saturated rock as functions of the porosity, the elastic moduli of the dry skeleton, the bulk modulus of the solid grain material, and the bulk modulus (incompressibility) of the pore fluid.

However, such explicit yet general expressions are not known for reservoirs with aligned fractures.

* Tel.: +61-8-9266-7359; fax: +61-8-9266-3407.
E-mail address: boris.gurevich@geophy.curtin.edu.au (B. Gurevich).

0926-9851/$ - see front matter © 2003 Elsevier B.V. All rights reserved.
doi:10.1016/j.jappgeo.2002.11.002

Several treatments of the porous media with aligned fractures have been developed in recent years (Thomsen, 1995; Hudson et al., 1996, 2001). However, these treatments are based on a specific and idealized fracture geometry (the so-called penny-shaped crack), and are restricted to small crack densities.

More general relationships between dry and fluid-saturated properties of fractured porous media can be based on the general linear-slip model of the medium with parallel fractures (Schoenberg and Douma, 1988; Schoenberg and Sayers, 1995). This model, based on physically intuitive relations between stress and discontinuity in displacement across the fracture, is formulated in terms of excess compliance due to the presence of fractures, and requires no assumptions about the microstructure or microgeometry of the fractures.

Suppose that the dry porous and fractured skeleton of the rock can be described by the general linear-slip model. In the low-frequency limit, the medium described by the linear-slip model is equivalent to a transversely isotropic (TI) elastic medium. Therefore, the same medium saturated with a fluid is also a TI medium, whose elastic properties may be expressed through the anisotropic Gassmann equations (Gassmann, 1951; Brown and Korringa, 1975; Xu, 1998; Cardona, 2002).

In this paper, we use equations of anisotropic poroelasticity applicable to TI media to derive explicit expressions for the low-frequency elastic constants and anisotropy parameters of the fractured porous medium saturated with a given fluid. The five elastic constants of the resultant TI medium are derived as explicit expressions in the properties of the dry (isotropic) background porous matrix, fracture properties (normal and shear excess compliances), and fluid bulk modulus.

2. Linear slip model for the dry skeleton

We assume that the dry rock is a spatially homogeneous and isotropic porous rock (host rock) permeated by a set of parallel fractures. The host rock is assumed to be made up of a single isotropic elastic grain material with the bulk modulus K_g. The host rock is characterized by porosity ϕ_p and Lamé constants λ and μ, so that its stiffness matrix can be written in the form

$$\mathbf{c}_b = \begin{pmatrix} \lambda+2\mu & \lambda & \lambda & 0 & 0 & 0 \\ \lambda & \lambda+2\mu & \lambda & 0 & 0 & 0 \\ \lambda & \lambda & \lambda+2\mu & 0 & 0 & 0 \\ 0 & 0 & 0 & \mu & 0 & 0 \\ 0 & 0 & 0 & 0 & \mu & 0 \\ 0 & 0 & 0 & 0 & 0 & \mu \end{pmatrix}.$$

The host rock is permeated by a set of parallel fractures which are described by the linear slip model (Schoenberg and Douma, 1988; Schoenberg and Sayers, 1995). According to this model, in the limit of low frequencies, an elastic medium permeated by a single set of parallel fractures can be characterized by the compliance matrix

$$\mathbf{s}^0 = \mathbf{s}_b + \mathbf{s}_c, \tag{1}$$

where $\mathbf{s}_b$ is the compliance matrix (inverse of stiffness matrix $\mathbf{c}_b$) of the host medium and $\mathbf{s}_c$ is the excess compliance matrix associated with the fractures (cracks). Here and below, we assume that the fracture set is rotationally invariant about the x_1 axis, which is normal to the fracture plane. In this case, the excess compliance matrix can be expressed in the form (Schoenberg and Sayers, 1995)

$$\mathbf{s}_c = \begin{pmatrix} Z_N & 0 & 0 & 0 & 0 & 0 \\ 0 & 0 & 0 & 0 & 0 & 0 \\ 0 & 0 & 0 & 0 & 0 & 0 \\ 0 & 0 & 0 & 0 & 0 & 0 \\ 0 & 0 & 0 & 0 & Z_T & 0 \\ 0 & 0 & 0 & 0 & 0 & Z_T \end{pmatrix}, \tag{2}$$

where Z_N and Z_T denote the so-called normal and shear excess compliances caused by the presence of fractures.

The compliance and stiffness matrices given by Eq. (1) describe an effective medium which is transversely isotropic (TI) with the symmetry axis x_1. Although general TI media are defined by five independent elastic parameters (c^0_{11}, c^0_{33}, c^0_{13}, c^0_{44}, and $c^0_{55}=c^0_{66}$), the elastic properties of an isotropic medium with rotationally invariant parallel fractures are fully described by four parameters: two elastic constants of the host medium λ and μ, and two excess compliances Z_N and Z_T. Consequently, its stiffness matrix $\mathbf{c}^0$ (inverse of $\mathbf{s}^0$) represents a special case of the general compliance matrix for a TI medium in that the five elastic constants are not independent but are related by the equation (Schoenberg and Sayers, 1995):

$$c^0_{11}c^0_{33}-(c^0_{13})^2-2c^0_{44}(c^0_{11}+c^0_{13})=0. \tag{3}$$

3. The effect of the fluid

Our aim is to study the effect of the saturating fluid on the elastic properties of the fractured porous rock. This cannot be done using standard isotropic Gassmann equations. In his landmark paper, Gassmann (1951) presented analogous equations also for the media with anisotropic skeleton made up of a single isotropic elastic grain material. For this case, the relationship between the dry and saturated elastic moduli of the rock can be written in the form

$$c^{sat}_{ij}=c^0_{ij}+\alpha_i\alpha_j M,\ \ i,j=1,\dots 6 \tag{4}$$

where

$$\alpha_m=1-\frac{\sum_{n=1}^{3}c^0_{mn}}{3K_g}, \tag{5}$$

for m = 1,2, and 3, $\alpha_4=\alpha_5=\alpha_6=0$, and the scalar M is the direct analog of Gassmann's pore space modulus:

$$M=\frac{K_g}{\left(1-\frac{K^*}{K_g}\right)-\phi\left(1-\frac{K_g}{K_f}\right)}. \tag{6}$$

In Eq. (6), ϕ is the overall porosity of the porous fractured rock (sum of background porosity ϕ_p and fracture porosity ϕ_c) and K^* denotes the so-called generalized drained bulk modulus, which is defined as

$$K^*=\frac{1}{9}\sum_{i=1}^{3}\sum_{j=1}^{3}c^0_{ij}. \tag{7}$$

A different but entirely equivalent formulation of the anisotropic Gassmann equations has been derived by Brown and Korringa (1975), who also extended them to account for microheterogeneous and anisotropic grain material. Equations of Brown and Korringa (1975) were used by Cardona (2002) to develop a model for fluid substitution in fractured porous media, which is similar to the one presented in this paper.

As discussed in the previous section, our dry rock is transversely isotropic, in which case Eq. (5) yields:

$$\alpha_1=1-\frac{c^0_{11}+2c^0_{13}}{3K_g}, \tag{8}$$

$$\alpha_2=\alpha_3=1-\frac{c^0_{13}+c^0_{23}+c^0_{33}}{3K_g} \tag{9}$$

and $\alpha_4=\alpha_5=\alpha_6=0$.

To apply these relationships to our porous fractured medium, we first invert matrix $\mathbf{s}^0$ to obtain dry rock stiffnesses c^0_{ij}, and then substitute these stiffnesses into Eqs. (7)–(9) to obtain

$$K^*=K\left(1-\frac{K}{\lambda+2\mu}\Delta_N\right), \tag{10}$$

$$\alpha_1=1-\frac{K}{K_g}(1-\Delta_N)=\alpha_0+\frac{K}{K_g}\Delta_N, \tag{11}$$

$$\alpha_2=\alpha_3=\alpha_0+\frac{K\lambda}{K_g(\lambda+2\mu)}\Delta_N, \tag{12}$$

where $K=\lambda+2\mu/3$ is the bulk modulus of the dry host rock, $\alpha_0=1-K/K_g$, while

$$\Delta_N=\frac{(\lambda+2\mu)Z_N}{1+(\lambda+2\mu)Z_N} \tag{13}$$

and

$$\Delta_T=\frac{\mu Z_T}{1+\mu Z_T} \tag{14}$$

denote dimensionless fracture weaknesses.

Finally, substituting dry-rock stiffnesses into Eq. (4), we obtain the stiffnesses of the saturated fractured porous medium as explicit expressions in the moduli of the host rock, fracture weaknesses, and fluid modulus:

$$c_{11}^{sat}=\frac{L}{D}\left\{d_1\theta+\frac{K_f}{\phi K_g L}\left[L_1\alpha' -\frac{16}{9}\frac{\mu^2\alpha_0}{L}\Delta_N\right]\right\}, \tag{15}$$

$$c_{33}^{sat}=\frac{L}{D}\left\{d_2\theta+\frac{K_f}{\phi K_g L}\left[L_1\alpha' -\frac{4}{9}\frac{\mu^2\alpha_0}{L}\Delta_N\right]\right\}, \tag{16}$$

$$c_{13}^{sat}=\frac{\lambda}{D}\left\{d_1\theta+\frac{K_f}{\phi K_g \lambda}\left[\lambda_1\alpha' +\frac{8}{9}\frac{\mu^2\alpha_0}{L}\Delta_N\right]\right\}, \tag{17}$$

$$c_{44}^{sat}=\mu, \tag{18}$$

$$c_{55}^{sat}=\mu(1-\Delta_T), \tag{19}$$

where

$$D=1+\frac{K_f}{K_g\phi}\left(\alpha_0-\phi+\frac{K^2\Delta_N}{K_g L}\right), \tag{20}$$

$$\theta=1-\frac{K_f}{K_g},\ \alpha' =\alpha_0+\frac{K^2}{K_g L}\Delta_N, \tag{21}$$

$$L_1=K_g+\frac{4}{3}\mu,\ \lambda_1=K_g-\frac{2}{3}\mu, \tag{22}$$

$$d_1=1-\Delta_N,\ d_2=1-\frac{\lambda^2}{L_2}\Delta_N. \tag{23}$$

We see that c_{44}^{sat} and c_{55}^{sat} are not affected by the fluid. For compactness, in Eqs. (15)–(19), we use four elastic constants λ, μ, $K=\lambda+2\mu/3$, and $L=\lambda+2\mu$ of the dry isotropic host rock, while only two of these constants are, of course, independent.

Eqs. (15)–(19) provide a complete description of the elastic properties of the saturated rock with aligned fractures. Note that no approximations have been made with respect to the degree of fracturing (fracture weakness or fracture density) or fluid modulus, as is often done in studies of fluid effects in fractured rocks (Thomsen, 1995; Hudson et al., 1996, 2001).

4. Anisotropy parameters

One of the key issues related to elastic properties in fractured media is the effect of pore fluid on anisotropy. The degree of anisotropy of a TI medium is described by Thomsen's (1986) parameters ϵ, δ, and γ, which describe the variation of compressional and shear velocities as a function of polar angle with respect to symmetry axis:

$$\epsilon=\frac{c_{33}-c_{11}}{2c_{11}}, \tag{24}$$

$$\gamma=\frac{c_{44}-c_{55}}{2c_{55}}, \tag{25}$$

$$\delta=\frac{(c_{13}+c_{55})^2-(c_{11}-c_{55})^2}{2c_{11}(c_{11}-c_{55})}. \tag{26}$$

For a fractured medium with an isotropic background and parallel fractures, Thomsen's (1986)

parameters can be expressed in terms of normal and shear compliances. Since the properties of this medium are defined by four rather than five parameters, the three anisotropy parameters are not independent, and two parameters, say, ϵ and γ, are sufficient to characterize the anisotropy of that medium:

$$\epsilon^0 = \frac{2\mu(\lambda+\mu)\Delta_N}{L^2(1-\Delta_N)}, \tag{27}$$

$$\gamma^0 = \frac{\Delta_T}{2(1-\Delta_T)}, \tag{28}$$

with δ fully determined by ϵ and γ. In case of small anisotropy $\epsilon^0 \ll 1$, $\gamma^0 \ll 1$, this relationship is

$$\delta^0 = 2(1-v)\epsilon^0 - 2\frac{1-2v}{1-v}\gamma^0, \tag{29}$$

where $v=(3K-2\mu)/2(3K+\mu)$ is Poisson's ratio of the dry background medium. If these parameters are obtained, for instance, from measurements of seismic wave velocities, fracture weaknesses can be estimated by solving Eqs. (27) and (28) for Δ_N and Δ_T:

$$\Delta_N = \frac{\epsilon(\lambda+2\mu)^2}{\epsilon(\lambda+2\mu)^2 + 2\mu(\lambda+\mu)}. \tag{30}$$

and

$$\Delta_T = \frac{2\gamma}{1+2\gamma}. \tag{31}$$

In turn, fracture compliances can be calculated by inverting Eqs. (13) and (14) for Z_N and Z_T, and substituting Δ_N and Δ_T from Eqs. (30) and (31):

$$Z_N = \frac{\epsilon(\lambda+2\mu)}{2\mu(\lambda+\mu)}, \quad Z_T = \frac{2\gamma}{\mu}. \tag{32}$$

For a saturated rock, the anisotropy parameters ϵ and γ can be obtained by substituting saturated rock stiffnesses as given by Eqs. (15)–(19) into Eqs. (24) and (25):

$$\epsilon^{sat} = \epsilon^0 \frac{1 - \frac{K_f}{K_g} + \frac{1}{3}\frac{K_f\mu\alpha_0}{\phi K_g(\mu+\lambda)}}{1 - \frac{K_f}{K_g} + \frac{K_f}{(1-\Delta_N)\phi K_g L}\left[\left(K_g + \frac{4}{3}\mu\right)\left(\alpha_0 + \frac{K^2}{K_g L}\Delta_N\right) - \frac{16}{9}\frac{\mu^2\alpha_0}{L}\Delta_N\right]}, \tag{33}$$

$$\gamma^{sat} = \gamma^0 = \frac{\Delta_T}{2(1-\Delta_T)}, \tag{34}$$

where ϵ^0 and γ^0 are dry anisotropy parameters given by Eqs. (27) and (28), respectively.

Eq. (33) can be compared with the results of Thomsen (1995) who derived expressions for anisotropy parameters of a porous rock with aligned penny-shaped cracks. The result of Thomsen (1995) can be written in the form

$$\epsilon^T = \frac{8e}{3}\frac{L}{L^{sat}}\frac{(K^{sat}+\mu/3)}{(K+\mu/3)} \times \frac{1-\frac{K_f}{K_g}}{1 - \frac{K_f}{K_g} + \frac{K_f}{\phi}\left[\frac{\alpha_0}{K} + \frac{4e}{3}\frac{L}{\mu}\frac{1}{K+\mu/3}\right]}. \tag{35}$$

In Eq. (35), e is the crack density, which is related to the crack porosity ϕ_c and aspect ratio a of the spheroidal crack (ratio of the minor to the major axis of the spheroid) by

$$e = \frac{3\phi_c}{4\pi a}, \tag{36}$$

K^{sat} is the undrained (Gassmann) bulk modulus of the porous uncracked host rock

$$K^{sat} = K + \alpha_0^2 M_0 \tag{37}$$

and $L^{sat}=K^{sat}+4\mu/3$. To compare our Eq. (33) with Thomson's results, we need to express fracture compliances or weaknesses in the linear-slip model for the

particular case of penny-shaped cracks. Such relationships have been derived by Schoenberg and Douma (1988):

$$Z_N = \frac{4L}{3\mu(L-\mu)}e, \tag{38}$$

or

$$\Delta_N = \frac{4e(K+4\mu/3)^2}{4e(K+4\mu/3)^2 + 3\mu(K+\mu/3)}. \tag{39}$$

Substitution of Δ_N as given by Eq. (39) into Eq. (33) for small crack densities yields

$$\epsilon^{sat} = \frac{8e}{3}\frac{1-\frac{K_f}{K_g}\left(1-\frac{\alpha_0}{3\phi}\frac{\mu}{K+\mu/3}\right)}{1-\frac{K_f}{K_g}+\frac{K_f}{\phi}\left[\frac{K_g+4\mu/3}{K_gL}\alpha_0+\frac{4eL}{3\mu}\frac{1}{K+\mu/3}\right]}. \tag{40}$$

Thomsen's (1995) result (Eq. (35)) and our result (Eq. (40)) are very similar but are not identical. They coincide for the case when $K_f \ll K_g$, while the porosity is somewhat small so that the bulk modulus of the dry host medium is close to that of the grain material, $K \approx K_g$. However, in other cases, the two expressions give slightly different results. One of the ways to analyze the effect of background porosity and fluid on the elastic tensor is to represent the compliance matrix $\mathbf{s}^{sat}$ (inverse of $\mathbf{c}^{sat}$) in the form similar to Eq. (1): as a sum of an isotropic part and fracture-related part:

$$\mathbf{s}^{sat} = \mathbf{s}_g + \mathbf{s}_c^{sat}. \tag{41}$$

The isotropic part $\mathbf{s}_g$ corresponds to the medium without fractures, and thus can be easily obtained from isotropic Gassmann equations. The elements of fracture compliance matrix $\mathbf{s}_c^{sat}$ are the effective fracture compliances for the saturated fractures that can be obtained by substituting anisotropy parameters ϵ and γ as given by Eqs. (33) and (34) into Eq. (32) and replacing λ with its undrained (Gassmann) equivalent λ^{sat}:

$$\lambda^{sat} \equiv L^{sat} - \mu \equiv \lambda + \alpha_0^2 M_0, \tag{42}$$

where M_0 is given by Eq. (6) with $K^* = K$ and $\phi = \phi_p$. This can be written in the form

$$Z_N^{sat} = Z_N \frac{L^{sat}(\lambda+\mu)\epsilon^{sat}}{L(\lambda^{sat}+\mu)\epsilon^0}, \tag{43}$$

$$Z_T^{sat} = Z_T, \tag{44}$$

whereas before Z_N and Z_T represent dry fracture compliances, and ϵ^{sat} is given by Eq. (33). Together with Eq. (33), Eq. (43) shows how effective excess fracture compliance changes with fluid saturation and background porosity.

5. Analysis of the derived equations

5.1. Gassmann consistency

For non-fractured rock setting fracture weaknesses Δ_N and Δ_T to zero yields

$$c_{11}^{sat} = c_{33}^{sat} = L^{sat} \equiv L + \alpha_0^2 M_0, \tag{45}$$

$$c_{44}^{sat} = c_{55}^{sat} = \mu, \tag{46}$$

where M_0 is given by Eq. (6) with $K^* = K$,

$$M_0 = \frac{K_g}{\left(1-\frac{K}{K_g}\right)-\phi_p\left(1-\frac{K_g}{K_f}\right)} = \frac{1}{\frac{\alpha_0-\phi_p}{K_g}+\frac{\phi_p}{K_f}} = \frac{K_f}{\phi_p\left(1+\frac{\alpha_0-\phi_p}{\phi_p}\frac{K_f}{K_g}\right)}. \tag{47}$$

Eqs. (45) and (46) are equivalent to classical isotropic Gassmann equations and describe an isotropic fluid-saturated porous medium without fractures.

5.2. Properties of background and fracture porosities

The general Eqs. (15)–(19) provide expressions for saturated stiffnesses of any fractured porous rock as long as fractures in the dry skeleton can be described by a linear slip model (Eq. (1)). However, division of the total porosity into background porosity ϕ_p and fracture porosity ϕ_c allows us to derive more specific equations valid for typical reservoir conditions.

First, following Thomsen (1995), we assume that the background porosity is formed by so-called "equant" pores, that is, pores with aspect ratio of order 1. Such porosity is typical for clastic or granular reservoirs. As known from mechanics of composite materials (Christensen, 1979), of all possible pore shapes, such equant pores have a minimum softening effect on the overall elastic properties of the porous material, and are therefore often referred to as hard porosity (Mavko and Jizba, 1991). The softening effect of porosity is expressed via the parameter $\alpha_0 = 1 - K/K_g$, which in the case of equant porosity is of the same order of magnitude as the porosity itself, $\alpha_0/\phi_p = O(1)$. Moreover, for typical rocks, α_0 is usually two to four times greater than ϕ_p, so that

$$(\alpha_0 - \phi_p)/\phi_p = O(1). \tag{48}$$

In contrast to background porosity, the fracture porosity ϕ_c will be assumed to consist of crack-like thin pores, which behave much like oblate spheroids (penny-shaped cracks) with very small aspect ratio (<0.01). This shape makes such pores very compliant (soft porosity, Mavko and Jizba, 1991), and they have a significant effect on the effective elastic properties of the material even if present in relatively small quantities. In our notation, the softening effect of fracture porosity on dry elastic properties is described by dimensionless weaknesses Δ_N and Δ_T. The fact that fracture porosity is a "soft porosity" can be written as $\Delta_N \gg \phi_c$, $\Delta_T \gg \phi_c$. Following the analysis of Schoenberg and Sayers (1995), we will assume that fracture compliances Z_N and Z_T are of the same order of magnitude (though not necessarily equal), $Z_N/Z_T = O(1)$. This means that $\Delta_N/g\Delta_T = O(1)$, where $g=(\lambda+2\mu)/\mu$, and thus

$$\phi_c \ll \Delta_T < \Delta_N < 1. \tag{49}$$

In addition, we will assume for simplicity that the bulk modulus of the fluid is small compared with that of the grains, $K_f \ll K_g$. This does not mean that all the terms containing K_f/K_g can be neglected, as these terms may contain combinations like Δ_N/ϕ, which may be very large. Moreover, to be negligible, these terms must be small compared with terms containing Δ_N, which may themselves be small. Taking this into account, we can observe that the terms containing $\mu^2\alpha_0\Delta_N/L$ in the right-hand side of Eqs. (15)–(17) can always be neglected. Indeed, when the background medium is non-porous, $\phi_p = 0$ and $\alpha_0 = 0$. Conversely, when background porosity is large, this term is small because it is proportional to $\Delta_N K_f/K_g$. By neglecting the terms containing $\alpha_0\Delta_N K_f/K_g$, we can rewrite Eqs. (15)–(17) as

$$c_{11}^{sat} = \frac{L}{D}\left\{(1-\Delta_N)\theta + \frac{K_f}{\phi K_g L}\left(K_g + \frac{4}{3}\mu\right) \times \left(\alpha_0 + \frac{K^2}{K_g L}\Delta_N\right)\right\}, \tag{50}$$

$$c_{33}^{sat} = \frac{L}{D}\left\{\left(1 - \frac{\lambda^2}{L^2}\Delta_N\right)\theta + \frac{K_f}{\phi K_g L}\left(K_g + \frac{4}{3}\mu\right) \times \left(\alpha_0 + \frac{K^2}{K_g L}\Delta_N\right)\right\}, \tag{51}$$

$$c_{13}^{sat} = \frac{\lambda}{D}\left\{(1-\Delta_N)\theta + \frac{K_f}{\phi K_g \lambda}\left(K_g - \frac{2}{3}\mu\right) \times \left(\alpha_0 + \frac{K^2}{K_g L}\Delta_N\right)\right\} \tag{52}$$

with $\theta = 1 - K_f/K_g$ and D given by Eq. (20). We can observe that equations for c_{11}^{sat} and c_{33}^{sat} are now identical, but for the factor λ^2/L^2, multiplying Δ_N in c_{33}^{sat} in the term which is not affected by the fluid. Therefore, the expression for ϵ^{sat} reduces to

$$\epsilon^{sat} = \frac{\epsilon^0}{1 + \dfrac{K_f\left(K_g + \frac{4}{3}\mu\right)\left(\alpha_0 + \frac{K^2}{K_g L}\Delta_N\right)}{(1-\Delta_N)\phi(K_g - K_f)L}}, \tag{53}$$

The simplifications made in this section allow us to derive even simpler expressions for two important

special cases of a non-porous background and background with relatively large porosity.

5.3. Isolated fluid-filled fractures

If fractures are embedded in a non-porous background, the background porosity ϕ_p is zero (and hence $\phi=\phi_c$), while the elastic moduli of the dry isotropic host rock K and μ are equal to the moduli K_g and μ_g of the grain material, so that $\alpha_0 \equiv 1-K/K_g=0$.

Therefore, the elastic properties of the non-porous medium with parallel isolated fractures can be obtained by substituting $\phi=\phi_c$ and $\alpha_0=0$ into Eqs. (15)–19) and (33):

$$c_{11}^{sat}=\frac{L}{D}\left\{(1-\Delta_N)\left(1-\frac{K_f}{K_g}\right)+\frac{K_f}{\phi_c L}\Delta_N\right\}, \tag{54}$$

$$c_{33}^{sat}=\frac{L}{D}\left\{(1-\frac{\lambda^2}{L^2}\Delta_N)\left(1-\frac{K_f}{K_g}\right)+\frac{K_f}{\phi_c L}\Delta_N\right\}, \tag{55}$$

$$c_{13}^{sat}=\frac{\lambda}{D}\left\{(1-\Delta_N)\left(1-\frac{K_f}{K_g}\right)+\frac{K_f}{\phi_c L}\Delta_N\right\}, \tag{56}$$

with

$$D=1-\frac{K_f}{K_g}+\frac{K_f\Delta_N}{L_g\phi_c} \tag{57}$$

and

$$L_g=K_g+4\mu_g/3,\ \lambda_g=K_g-2\mu_g/3.$$

For the anisotropy parameter ϵ^{is}, we have

$$\epsilon^{is}=\epsilon^0\frac{1-\frac{K_f}{K_g}}{1-\frac{K_f}{K_g}+\frac{K_f}{L_g}\frac{\Delta_N}{\phi_c(1-\Delta_N)}}=\frac{\epsilon^0}{1+\frac{K_f K_g}{(K_g-K_f)L_g}\frac{\Delta_N}{\phi_c(1-\Delta_N)}}. \tag{58}$$

Further evaluation of this result requires a relationship between normal fracture weakness for the dry rock Δ_N and fracture porosity ϕ_c. Such a relationship depends on the microgeometry of the fractures. In particular, for the popular model of aligned penny-shaped cracks (Hudson, 1980, 1981; Nishizawa, 1982), we can use fracture parameters given by Eqs. (38) and (39). This yields, for small crack densities,

$$\epsilon^{is}=\frac{8e}{3}\frac{1}{1+\frac{1}{\pi a}\frac{K_g+4\mu_g/3}{\mu_g}\frac{K_f}{K_g+\mu_g/3}\left(1-\frac{K_f}{K_g}\right)^{-1}}. \tag{59}$$

Eq. (59) is identical to the result of Thomsen (1995) for low concentrations of penny-shaped cracks; see also Hudson et al. (2001).

For isolated fractures, the effective normal fracture compliance as given by Eq. (43) can be written as

$$Z_N^{sat}=\frac{Z_N}{1+\frac{K_f\Delta_N}{L_g\phi_c(1-\Delta_N)}\left(1-\frac{K_f}{K_g}\right)^{-1}}. \tag{60}$$

If the fluid is very compressible, so that $K_f/L_g\to 0$ then also $Z_N^{sat}=Z_N$, as one would expect. If, however, the fluid is liquid, then

$$Z_N^{is}=Z_N\frac{L_g\phi_c}{K_f\Delta_N}\left(1-\frac{K_f}{K_g}\right)\ll Z_N, \tag{61}$$

and therefore $Z_N^{sat}\ll Z_T^{sat}=Z_T$. This is a well-known property of fractured non-porous media (Schoenberg and Douma, 1988).

5.4. Effect of background porosity

The central issue in this paper is the effect of background porosity on the elastic properties of the fluid-saturated fractured rock. As we assume that the background porosity is formed by equant pores, it is clear that small amounts of background porosity (on the scale of ϕ_c) have virtually no effect on the overall elastic properties of the rock. We will therefore assume in this section that $\phi_p\gg\phi_c$.

With these assumptions and conditions (Eqs. (48) and (49)), the term Δ_N/ϕ is of order 1, and when

multiplied by K_f/K_g can be neglected. Thus Eqs. (50)–(52) can be further simplified and re-arranged to give

$$c_{11}^{sat} = L + \alpha^2 \frac{K_f}{\phi_p D_0} - \frac{L}{D_0}\Delta_N = L^{sat} - \frac{L}{D_0}\Delta_N, \quad (62)$$

$$c_{33}^{sat} = L + \alpha^2 \frac{K_f}{\phi_p D_0} - \frac{\lambda^2}{LD_0}\Delta_N = L^{sat} - \frac{\lambda^2}{LD_0}\Delta_N, \quad (63)$$

$$c_{13}^{sat} = \lambda + \alpha^2 \frac{K_f}{\phi_p D_0} - \frac{\lambda}{D_0}\Delta_N = \lambda^{sat} - \frac{L}{D_0}\Delta_N, \quad (64)$$

where

$$D_0 = 1 + \frac{\alpha_0 - \phi_p}{\phi_p}\frac{K_f}{K_g} = \frac{M_0\phi_p}{K_f}. \quad (65)$$

The corresponding equation for anisotropy parameter ϵ^{sat} is

$$\epsilon^{sat} = \frac{2\mu(\lambda+\mu)\Delta_N}{D_0 L(L^{sat} - L\Delta_N/D_0)} = \epsilon^0 \frac{L}{L^{sat}}\frac{1-\Delta_N}{D_0}\left(1 - \frac{L\Delta_N}{L^{sat}D_0}\right)^{-1}. \quad (66)$$

For weakly fractured media, $\Delta_N \ll 1$, we have

$$\epsilon^{sat} = \epsilon^0 \frac{L}{L^{sat}D_0}. \quad (67)$$

Finally, effective saturated fracture compliance can be obtained by substituting ϵ^{sat} as given by Eq. (67) into Eq. (43):

$$Z_N^{sat} = Z_N \frac{(\lambda+\mu)}{\lambda^{sat}+\mu}\frac{1-\Delta_N}{D_0}\left(1 - \frac{L\Delta_N}{L^{sat}D_0}\right)^{-1}, \quad (68)$$

or, for weak fracture anisotropy

$$Z_N^{sat} = Z_N \frac{(\lambda+\mu)}{D_0(\lambda^{sat}+\mu)}. \quad (69)$$

Eq. (69) shows that in the presence of background porosity, the saturated normal fracture compliance Z_N^{sat} is of the same order of magnitude as, but somewhat smaller than, the dry fracture compliance Z_N. Intuitive arguments as well as the analysis of Schoenberg and Douma (1988) based on the theoretical result of Thomsen published later in Thomsen (1995), Eq. (35), suggested that the presence of a non-zero background porosity $\phi_p \gg \phi_c$ tends to produce a non-zero normal fracture compliance, i.e., $0 < Z_N^{sat} < Z_T$. Eq. (69) provides a quantitative confirmation of this phenomenon.

5.5. Numerical illustration

The effect of background porosity on the anisotropy of the fractured medium is illustrated in Figs. 1–3. Numerical computations require elastic constants of the dry porous background rock as a function of porosity. For this purpose, we used empirical model of (Krief et al. (1990)):

$$K = (1-\alpha_0)K_g; \quad (70)$$

$$\mu = (1-\alpha_0)\mu_g; \quad (71)$$

with α_0 given by

$$\alpha_0 = 1 - (1-\phi_p)^{\frac{3}{1-\phi_p}}. \quad (72)$$

Fig. 1 shows the anisotropy parameter ϵ as a function of fluid bulk modulus K_f for different porosities. For each porosity, a different value of normal fracture compliance was chosen so as to produce the same value for $\epsilon^0 = 0.1$ for the dry medium and fracture porosity of 0.01%. (this corresponds to crack density of penny-shaped cracks equal to 0.0375). As described in this section, we see that at very low background porosities, ϵ^{sat} tends to zero as K_f increases. However, even for modest values of background porosity, ϵ^{sat} shows a much more gradual decrease with fluid modulus. Similar behaviour is observed for the effective excess normal fracture compliance Z_N^{sat} (Fig. 2). Interestingly, the decrease

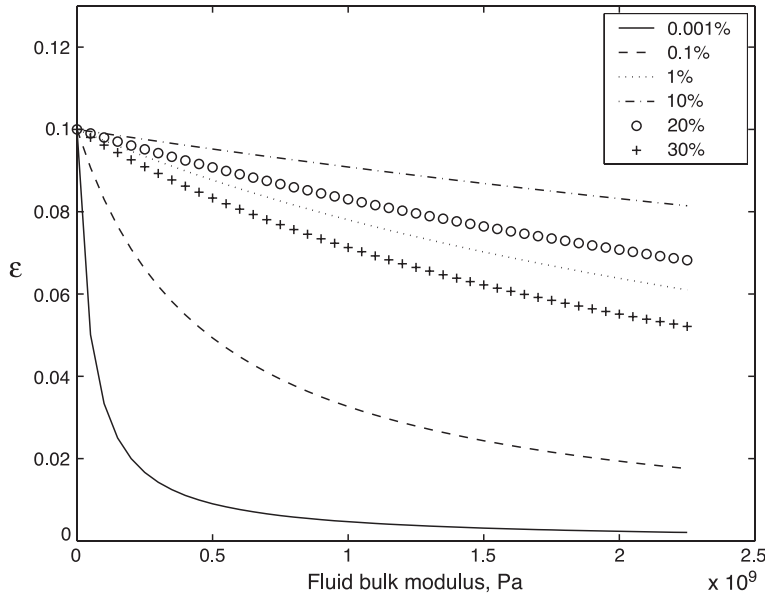

Fig. 1. *P*-wave anisotropy parameter ϵ versus fluid bulk modulus for different values of background porosity. For each porosity, the fracture compliances have been adjusted to provide the same value of $\epsilon = 0.1$ for the dry rock.

of both ϵ^{sat} and Z_N^{sat} with K_f is minimal at porosity around 10%, and then increases again.

Fig. 3 further examines this effect. It presents ϵ^{sat} as a function of background porosity ϕ_p for water-saturated rock ($K_f = 2.25 \times 10^9$ Pa). The solid line shows the full solution, Eq. (33), dashed line the asymptotic solution for large background porosity, Eq. (66), and dotted line Thomsen's (1995) solution, Eq. (35). We see that ϵ^{sat} is zero for zero background porosity, and sharply increases within a range of a few percent

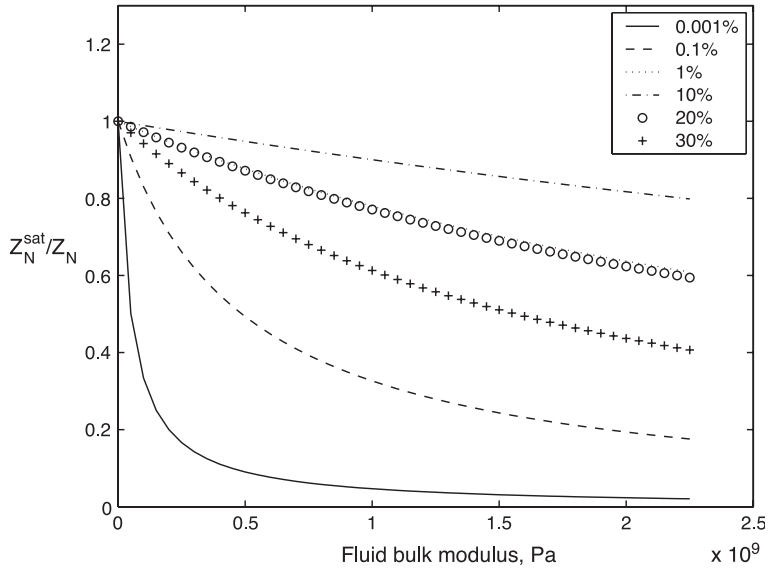

Fig. 2. The ratio of saturated-to-dry fracture compliances versus fluid bulk modulus for different values of the background porosity.

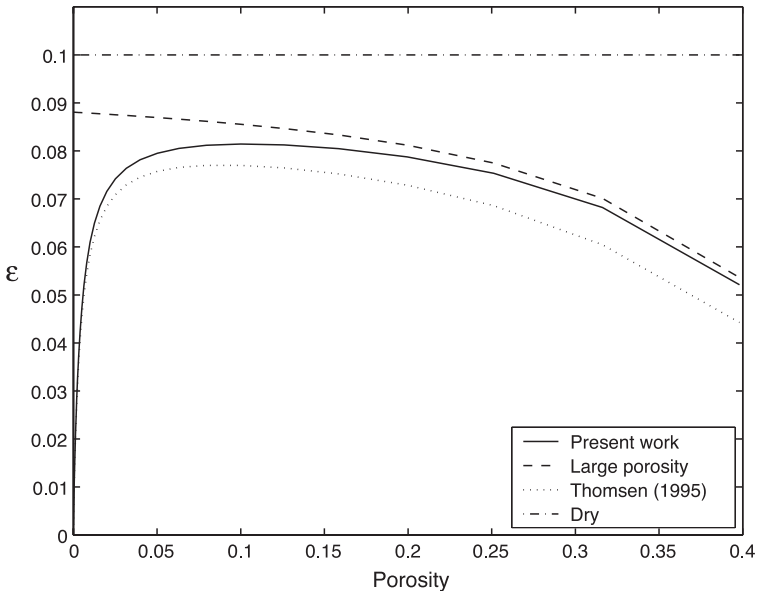

Fig. 3. *P*-wave anisotropy parameter ϵ versus background porosity as predicted by the anisotropic Gassmann theory, Eq. (33) (solid line), large-porosity approximation, Eq. (66) (dashed line), and Thomsen (1995) theory, Eq. (35) (dotted line). Dash–dotted line shows ϵ for the dry rock. For each porosity, the fracture compliances have been adjusted to provide the same value $\epsilon = 0.1$ for the dry rock.

porosity almost to ϵ^0, the value of ϵ for the dry medium. After that, the dependency of ϵ^{sat} on ϕ_p flattens out and is followed by a gradual decrease down to about half of ϵ^0, at background porosity of about 0.4.

As discussed by Thomsen (1995) and Hudson et al. (2001), the sharp increase of ϵ^{sat} results from the fact that when surrounded by (equant) pores, the fluid in the fracture has plenty of space around it to escape to when compressed, and therefore the fracture is almost as compliant as in the dry medium. In other words, stiffening of compliant pores by the fluid does not occur, as fluid can escape into the pores. Mathematically, this behaviour is best described by Eq. (53). The parameter that controls this transition is the ratio of the second to the first term in the denominator of the right-hand side of Eq. (53), which can be approximately written as

$$F = \frac{K_f K (K_g + 4\mu/3)\Delta_N}{K_g^2 L^2 \phi} \approx \frac{K_f \epsilon^0}{K_g \phi} = \frac{\phi_t}{\phi}, \qquad (73)$$

where $\phi_t = K_f \epsilon^0 / 2K_g$ is the characteristic porosity around which the sharpest rise of ϵ^{sat} with ϕ_p occurs. For $\phi_p \ll \phi_t$, the factor $F = \phi_t/(\phi_c + \phi_p)$ is very large, and thus ϵ^{sat} is close to zero. For $\phi_p \gg \phi_t$, the factor F becomes small, and the denominator in Eq. (53) is of order 1, which gives $\epsilon^{sat} = O(\epsilon^0)$. For our numerical example, $\epsilon^0 = 0.1$, $K_g = 40$ GPa, and the characteristic porosity ϕ_t is about 5%. This means that no more than 10% porosity provides enough space for the fluid to escape from the fracture. Note that for given grain and fluid bulk moduli, the characteristic porosity ϕ_t is chiefly controlled by the dry fracture weakness or degree of fracture anisotropy, and is unrelated to fracture porosity, which is much smaller (0.01%) in our case.

At background porosities several times greater than ϕ_t, the factor F becomes small, and a simple high-porosity approximation given by Eq. (66) or Eq. (67) can be used. The gradual decrease of ϵ^{sat} at higher background porosities is simply the result of fluid saturation; the more porous the rock, the greater the role of the saturating fluid in overall properties of the rock. Since the pore fluid is isotropic, it tends to reduce the overall degree of anisotropy of the rock.

5.6. Properties of stiffness and compliance matrices

Eqs. (43) and (44) show how non-zero elements of the excess compliance matrix $\mathbf{s}_c$ change in the pres-

ence of fluid. This implies that all other elements of that matrix remain zero. As was mentioned before, the fact that the compliance matrix can be expressed as a sum of an isotropic compliance matrix for the non-fractured rock plus an excess compliance matrix with only three diagonal elements other than zero requires that elements of the stiffness matrix satisfy Eq. (3). In order to prove that this representation is also valid for the saturated case, we need to calculate the left-hand side of Eq. (3) with the dry stiffnesses c_{ij}^0 replaced by the saturated stiffnesses given by Eqs. (15)–(19). After a straightforward, but cumbersome calculation, we arrive at the result that Eq. (3) does not hold for the saturated rock:

$$c_{11}^{\rm sat}c_{33}^{\rm sat}-(c_{13}^{\rm sat})^2-2c_{44}^{\rm sat}(c_{11}^{\rm sat}+c_{13}^{\rm sat})\neq 0. \tag{74}$$

This largely unexpected result means that the compliance matrix for the saturated fractured medium with background porosity cannot be represented by the sum of an isotropic matrix and an excess compliance matrix of the form given by Eq. (2). One can still obtain the excess compliance matrix $\mathbf{s}_{\rm c}^{\rm sat}$ as a difference between the compliance matrix $\mathbf{s}^{\rm sat}$ and the isotropic compliance matrix $\mathbf{s}_{\rm g}$ obtained from dry compliances using isotropic Gassmann equations. However, such an excess compliance matrix will no longer have a form given by Eq. (2), but will have other non-zero elements:

$$\mathbf{s}_{\rm c}^{\rm sat}=\begin{pmatrix} Z_{\rm N}^{\rm sat}+\delta S_{11} & \delta S_{13} & \delta S_{13} & 0 & 0 & 0\\ \delta S_{13} & \delta S_{33} & \delta S_{23} & 0 & 0 & 0\\ \delta S_{13} & \delta S_{23} & \delta S_{33} & 0 & 0 & 0\\ 0 & 0 & 0 & 0 & 0 & 0\\ 0 & 0 & 0 & 0 & Z_{\rm T} & 0\\ 0 & 0 & 0 & 0 & 0 & Z_{\rm T} \end{pmatrix}.$$

where all quantities δS_{ij} are given by expressions that for small background porosity are proportional to the combination $\alpha_0 Z_{\rm N} K_{\rm f}$. Therefore, these quantities vanish for dry rocks, for rocks with zero background porosity (in which case $\alpha_0=0$) and, obviously, for non-fractured media. However, in the presence of fractures, background porosity, and fluid all δS_{ij} are non-zero.

This result contradicts the existing view that background porosity only influences one element of the upper-left quarter of excess compliance matrix $Z_{\rm N}$. The non-zero effect of background porosity on other compliances can be explained by the flow of fluids between pores and fractures. Indeed, if we compress the rock with no background porosity along x_3 or x_2 axis, its compliance is not affected by the fractures normal to x_1. However, if the rock also contains pores that are in hydraulic equilibrium with the fractures, the fluid will squeeze from pores into fractures, thus affecting the corresponding compliance. The hydraulic equilibrium is assured by the use of a low-frequency approximation, and an assumption of a non-zero permeability.

Thus, the saturated porous and fractured porous medium can no longer be described by four parameters (two elastic constants of the background and two excess compliances), but requires all five parameters that describe a general TI medium. It is therefore not sufficient to describe its anisotropy by ϵ and γ only; that is, the δ parameter is now an independent parameter. Expression for δ in the case of weak anisotropy can be obtained by substituting saturated stiffnesses given by Eqs. (18), (19), (62)–(64) into Eq. (26) and retaining only terms linear in $\Delta_{\rm N}$ and $\Delta_{\rm T}$. This yields:

$$\delta^{\rm sat}=\frac{2\mu}{L^{\rm sat}}(D_0^{-1}\Delta_{\rm N}-\Delta_{\rm T}), \tag{75}$$

or, in terms of $\epsilon^{\rm sat}$ and $\gamma^{\rm sat}$,

$$\delta^{\rm sat}=2(1-v)\epsilon^{\rm sat}-2\frac{1-2v^{\rm sat}}{1-v^{\rm sat}}\gamma^{\rm sat}, \tag{76}$$

where $v^{\rm sat}$ is Poisson's ratio of the saturated background medium, and $\gamma^{\rm sat}$ is given as before by Eq. (34). Expression for δ given by Eq. (76) differs from the value of δ that satisfies the requirement (expressed by Eqs. (3) and (29)).

For the saturated medium an equivalent equation would be

$$\delta^{\rm sat}=2(1-v^{\rm sat})\epsilon^{\rm sat}-2\frac{1-2v^{\rm sat}}{1-v^{\rm sat}}\gamma^{\rm sat}. \tag{77}$$

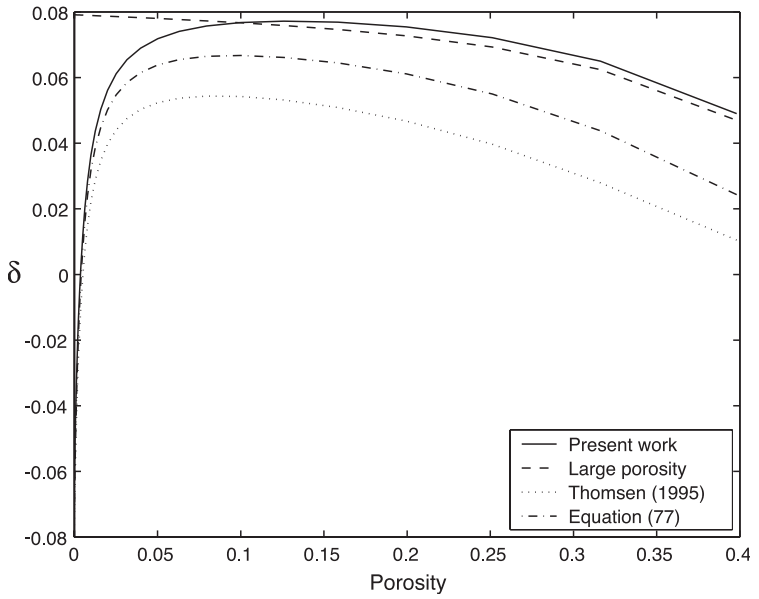

Fig. 4. Anisotropy parameter δ versus background porosity as predicted by the anisotropic Gassmann theory, Eqs. 62–64 (solid line), large-porosity approximation, Eq. (75) (dashed line), Thomsen's (1995) work (dotted line), and Eq. (77), with ϵ and γ obtained from exact Eqs. 62–64 (dash–dotted line).

Eq. (76) differs from Eq. (77) by the use of dry, rather than saturated, Poisson ratio in the term that multiplies ϵ^{sat}. Obviously, for large porosity, the difference may be significant. This is demonstrated by Fig. 4, which shows δ versus porosity corresponding to anisotropic Gassmann Eqs. (62)–(64) (solid line), large porosity/weak anisotropy approximation, Eq. (75) (dashed line), Thomsen's (1995) work (dotted line), and Eq. (77), with ϵ and γ obtained from exact Eqs. (62)–(64) (dash–dotted line).

An important implication of the analysis given in this section is that δ as given by Eq. (76) is not fully defined by the elastic constants of the saturated background medium plus ϵ^{sat} and γ^{sat}, but also depends on background porosity (through the difference between dry and saturated Poisson ratios of the background medium).

6. Higher frequencies

All the results derived above assume infinitely hydraulic equilibrium between pores and fractures, and are therefore valid for infinitely low frequencies. This regime is called "relaxed" by Mavko and Jizba (1991), and corresponds to the situation when the fluid diffusion length (Hudson et al., 2001)

$$J = \sqrt{\phi_p K_f \kappa / 2\eta\omega}. \tag{78}$$

(or the wavelength of Biot's slow wave, Biot, 1956a,b) is larger than the fracture size and fracture spacing,

$$c \ll a \ll J \tag{79}$$

(in Eq. (78), ω denotes frequency, κ the background permeability, and η the dynamic fluid viscosity).

At higher frequencies, the fluid will have no time to move between pores and fractures. This occurs when fracture opening becomes larger than the fluid diffusion length (Norris, 1993; Gurevich and Lopatnikov, 1995; Hudson et al., 2001), although fractures are still assumed to be smaller than the wavelength $2\pi v_p/\omega$:

$$J \ll c \ll 2\pi v_p/\omega \tag{80}$$

where ω is frequency. The regime defined by the condition (Eq. (80)) is called "unrelaxed" by Mavko

and Jizba (1991), and the corresponding frequencies are called moderately high by Thomsen (1995) and intermediate frequencies by Gurevich et al. (1998). In this regime, the flow between pores and fractures must be ignored, and the fractures should be treated as isolated fractures in the isotropic background whose elastic constants are given by the isotropic Gassmann equation. In particular, the expression for anisotropy parameter ϵ is identical to the one given by Eq. (58) with grain moduli K_g and μ_g replaced by the undrained modulus K^{sat} given by the Gassmann Eq. (37) and skeleton shear modulus μ, respectively:

$$\epsilon = \frac{2\mu(K^{sat}+\mu/3)\Delta_N}{(L^{sat})^2(1-\Delta_N)} \frac{1-\frac{K_f}{K_g}}{1-\frac{K_f}{K^{sat}}+\frac{K_f}{L^{sat}}\frac{\Delta_N}{\phi_c(1-\Delta_N)}}, \quad (81)$$

This result is equivalent to the corresponding result of Thomsen (1995) for moderately high frequencies.

7. Discussion

The above analysis shows how the low-frequency elastic properties of a fractured rock with a background porosity can be obtained using the Gassmann theory of poroelasticity. The main result is that a relatively small increase of background porosity (from zero to a few percent) leads to a sharp increase of *P*-wave anisotropy from a near-zero value for non-porous background to a value which is close to, but somewhat smaller than, *P*-wave anisotropy of the dry fractured rock. This result is qualitatively consistent with the prediction of the model of Thomsen (1995), which is based on the analysis of pressure equilibration in a system of penny-shaped cracks embedded in a porous background. Quantitative predictions of the anisotropic Gassmann and Thomsen (1995) model are identical for low concentrations of penny-shaped cracks, but differ slightly in the case of a porous background. The main qualitative difference is in the fact that the stiffness matrix predicted by the anisotropic Gassmann model does not obey the usual relationship (Eq. (3)) valid for dry or saturated rocks in a non-porous background. This means, in particular, that contrary to the prediction of Thomsen's (1995) model, the anisotropy parameter δ for the saturated rock is not fully defined by the elastic constants of the saturated background medium plus ϵ^{sat} and γ^{sat}, but also depends on the background porosity. A more detailed theoretical comparison of the anisotropic poroelasticity model and Thomsen's (1995) model is given by Cardona (2002), who introduced a model for elastic properties of a porous medium with aligned fractures based on the compliance-matrix formulation of Brown and Korringa (1975), which is entirely equivalent to the model presented here.

These results are valid in the low-frequency limit, when the fluid diffusion length is larger than the fracture size and fracture spacing. In the opposite limit of higher frequencies, when the fluid diffusion length is smaller than the fracture thickness, the fluid communication between pores and fractures can be neglected, and the results are equivalent to those derived for isolated fractures by Hudson (1981) and Thomsen (1995).

Another theoretical model of elastic properties of fractured media with background ("equant") porosity was developed by Hudson et al. (1996); see also corrections by Hudson et al. (2001). Unlike the Thomsen (1995) model and anisotropic Gassmann model proposed in the present paper, each of which have expressions only for limiting cases of low and high frequencies, Hudson et al. (1996) derived expressions for elastic moduli as continuous functions of frequency. In the high-frequency limit, these expressions are equivalent to the predictions of Thomsen (1995) and anisotropic Gassmann models. However, the Hudson et al. (1996) model differs substantially from these two models in the low-frequency limit, where it predicts that anisotropy is the same as for the dry rock, and does not depend on background porosity. This result apparently contradicts the known fact that for isolated liquid-filled cracks in a non-porous background, the anisotropy parameter ϵ is close to zero. However, this contradiction is resolved by the fact that the low-frequency limit can never be achieved for zero-porosity background. Indeed, as can be seen from Eq. (78), the diffusion length is proportional to background permeability, and is therefore zero for a non-porous background at any frequency. Therefore, similar to the anisotropic Gassmann and Thomsen (1995) models, the Hudson et al.

(1996) model predicts an increase of *P*-wave anisotropy with the increase of background porosity (from zero to a few percent). However, in contrast to those two models, this increase occurs at a given non-zero frequency, but not in the low-frequency limit, and is controlled by the permeability to viscosity ratio. Thus, the Hudson et al. (1996) model is not consistent with anisotropic Gassmann theory. As suggested by Hudson et al. (2001), this discrepancy might be the result of the fact that Hudson et al. (1996) is based on the analysis of a singe fracture in an infinite background medium, and therefore does not account for the interaction between inclusions which may be significant in the low-frequency limit when the diffusion length is larger than fracture spacing.

The analysis of elastic properties of the fractured rock with background porosity is most important when such porosity is significant (say, >8–10%), and thus can hold significant volumes of fluid. In this case, the general equations for elastic normal stiffnesses (Eq. (15)–(17)) reduce to Eqs. (62)–(64). For weakly anisotropic media, these results can also be recast in terms of anisotropy parameters which are given by Eqs. (34), (67), and (75). The main thing to note about these equations is that they are remarkably simple. As in many other situations in geophysics, the computations should always be performed using exact Eqs. (15)–(17), but simplified equations can be useful in providing physical insight and quick estimates. They can also be used as a basis for petrophysical inversion.

Finally, it should be noted all the results derived in this paper for both low and high frequencies (and corresponding results of Thomsen, 1995; Hudson et al., 1996, 2001) are only valid if the porous, non-fractured medium obeys the Gassmann equation. This is only true in the low-frequency regime of the Biot theory of poroelasticity (Biot, 1956a,b, 1962). For most reservoir rocks, this regime extends up to frequencies of 0.1–1 MHz.

8. Conclusions

The anisotropic Gassmann theory when combined with the linear-slip description of fractures provides a straightforward solution to the problem of elastic properties of a porous rock with parallel fractures. This solution provides explicit and exact analytical expressions of all elements of the effective stiffness matrix of such a rock in terms of elastic properties of the dry isotropic background, porosity, dry normal and shear excess fracture compliances, and bulk moduli of the grain material and the saturating fluid.

When recast in terms of Thomsen's (1986) anisotropy parameters, these expressions show that *P*-wave anisotropy parameter ϵ of the saturated fractured rock sharply increases from zero to a value close to its value for the dry rock as porosity increases from zero to a few percent. After reaching its maximum value at about 10% porosity, ϵ gradually decreases with porosity.

The shear wave anisotropy parameter γ is unaffected by the fluid and is equal to its value for the dry rock. The parameter δ is independent of ϵ and γ due to the fact that the compliance matrix of a fluid-saturated porous fractured medium is not equivalent to the compliance matrix of any equivalent solid medium with a single set of parallel fractures. This unexpected result is caused by the wave-induced flow of fluid between pores and fractures.

Acknowledgements

I thank Milovan Urosevic, Michael Schoenberg, Colin Sayers, and Andrey Bakulin for in-depth discussions that inspired this work, and Luke J. Brown for numerical calculations. I also thank Simon Tod and Reynaldo Cardona for the detailed review of the paper. The support of the Commonwealth Scientific Industrial Research Organisation (CSIRO), Center of Excellence for Exploration and Production Geophysics (CEEPG), Australian Petroleum Cooperative Research Centre (APCRC), and Curtin Reservoir Geophysics Consortium (CRGC) is gratefully acknowledged.

References

Biot, M.A., 1956a. Theory of propagation of elastic waves in a fluid-saturated porous solid: I. Low-frequency range. J. Acoust. Soc. Am. 28, 168–178.

Biot, M.A., 1956b. Theory of propagation of elastic waves in a fluid-saturated porous solid: II. Higher-frequency range. J. Acoust. Soc. Am. 28, 179–191.

Biot, M.A., 1962. Mechanics of deformation and acoustic propagation in porous media. J. Appl. Phys. 33, 1482–1498.

Brown, R.J.S., Korringa, J., 1975. On the dependence of the elastic properties of a porous rock on the compressibility of the pore fluid. Geophysics 40, 608–616.

Cardona, R., 2002. Two theories for fluid substitution in porous rocks with aligned cracks. 72nd Ann. Internat. Mtg., Soc. Expl. Geophys., Expanded Abstracts. Paper ANI, vol. 3.5.

Christensen, R.M., 1979. Mechanics of Composite Materials. Wiley-Interscience.

Gassmann, F., 1951. Über die elastizität poröser medien. Viertel. Naturforsch. Ges. Zürich 96, 1–23.

Gurevich, B., Lopatnikov, S.L., 1995. Velocity and attenuation of elastic waves in finely layered porous rocks. Geophys. J. Int. 121, 933–947.

Gurevich, B., Sadovnichaja, A.P., Lopatnikov, S.L., Shapiro, S.A., 1998. Scattering of a compressional wave in a poroelastic medium by an ellipsoidal inclusion. Geophys. J. Int. 133, 91–103.

Hudson, J.A., 1980. Overall properties of a cracked solid. Math. Proc. Camb. Philos. Soc. 88, 371–384.

Hudson, J.A., 1981. Wave speeds and attenuation of elastic waves in material containing cracks. Geophys. J. R. Astron. Soc. 64, 133–150.

Hudson, J.A., Liu, E., Crampin, S., 1996. The mechanical properties of materials with interconnected cracks and pores. Geophys. J. Int. 124, 105–112.

Hudson, J., Pointer, T., Liu, E., 2001. Effective-medium theories for fluid-saturated materials with aligned cracks. Geophys. Prospect. 49, 509–522.

Krief, M., Garat, J., Stellingwerff, J., Ventre, J., 1990. A petrophysical interpretation using the velocities of P and S waves (Full-Wave Sonic). Log Anal. , (5), 355–369.

Mavko, G., Jizba, D., 1991. Estimating grain-scale fluid effects on velocity dispersion in rocks. Geophysics 56, 1940–1949.

Nishizawa, O., 1982. Seismic velocity anisotropy in a medium containing oriented cracks—transversely isotropic case. J. Phys. Earth 30, 435–446.

Norris, A.N., 1993. Low-frequency dispersion and attenuation in partially saturated rocks. J. Acoust. Soc. Am. 94, 359–370.

Schoenberg, M., Douma, J., 1988. Elastic-wave propagation in media with parallel fractures and aligned cracks. Geophys. Prospect. 36, 571–590.

Schoenberg, M., Sayers, C.M., 1995. Seismic anisotropy of fractured rock. Geophysics 60, 204–211.

Thomsen, L., 1986. Weak elastic anisotropy. Geophysics 51, 1954–1966.

Thomsen, L., 1995. Elastic anisotropy due to aligned cracks in porous rock. Geophys. Prospect. 43, 805–829.

Xu, S., 1998. Modelling the effect of fluid communication on velocities in anisotropic porous rocks. Int. J. Solids Struct. 35, 4685–4704.